Oxidative removal of soluble divalent manganese ion by chlorine in the presence of superfine powdered activated carbon

Shun Saito [a, b], Yoshihiko Matsui [c]*, Yasuhiko Yamamoto [b], Shuhei Matsushita [d], Satoru Mima [b], Nobutaka Shirasaki [c], and Taku Matsushita [c]

[a] Graduate School of Engineering, Hokkaido University, N13W8, Sapporo 060-8628, Japan

[b] METAWATER Co., Ltd., Kandasuda-cho 1-25, Chiyoda-ku, Tokyo 101-8554, Japan

[c] Faculty of Engineering, Hokkaido University, N13W8, Sapporo 060-8628, Japan

[d] School of Engineering, Hokkaido University, N13W8, Sapporo 060-8628, Japan

* Corresponding author. Tel./fax: +81-11-706-7280

E-mail address: matsui@eng.hokudai.ac.jp

Research Highlights

- Superfine activated carbon and Cl_2 remove Mn(II) fast enough for practical purposes.
- Mn(II) is oxidized and precipitated on activated carbon in the presence of chlorine.
- External-film mass transfer is the rate-determining step of oxidative Mn(II) removal.
- The rate of Mn(II) removal follows pseudo-first-order reaction kinetics.
- Rate coefficient is in inverse proportion to as-is particle size of activated carbon.

Graphical Abstract

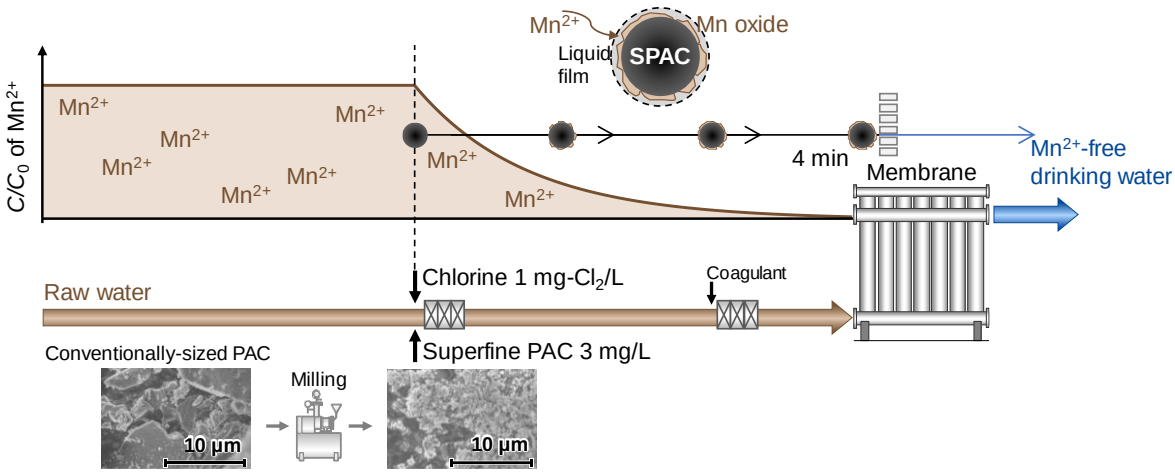

Abstract

Here, we examined the removal of soluble divalent manganese (Mn(II)) by combination treatment with superfine powdered activated carbon (SPAC) and free chlorine in a membrane filtration pilot plant and batch experiments. Removal rates >95 % were obtained with 3 mg/L SPAC, 1 mg/L chlorine, and a contact time of 4 min, meeting practical performance standards. Mn(II) was found to be oxidized and precipitated on the surface of the activated carbon particles by chlorine. The Mn(II) removal rate was fitted to pseudo-first-order reaction kinetics, and the rate coefficient changed in inverse proportion to as-is particle size, but not to true particle size. The rate coefficient was independent of both Mn(II) concentration, except at high Mn(II) concentration, and the chlorine concentrations tested. The rate-determining step of Mn(II) removal was confirmed to be external-film mass transfer, not chemical oxidation. Activated carbon was found to have a catalytic effect on the oxidation of Mn(II), but the effect was minimal for conventionally sized activated carbon. However, Mn(II) removal at feasible rates for practical application can be expected when the activated carbon particle diameter is reduced to several micrometers. Activated carbon with a particle size of around 1–2 μm may be the most appropriate for Mn(II) removal because particles below this size were aggregated, resulting in reduced removal efficiency.

Keywords

SPAC; catalysis; manganese; reaction kinetics; precipitation

1. Introduction

Several processes can be used to remove soluble divalent manganese (Mn(II)) in drinking water treatments. These include 1) oxidation of Mn(II) to an insoluble form by using strong oxidants, such as ozone, potassium permanganate, or chlorine dioxide, followed by solid–liquid separation (Carlson et al., 1997; Gregory and Carlson, 2003); 2) adsorption and catalytic oxidation on the surface of a metal oxide in the presence of free chlorine (Islam et al., 2010; Knocke et al., 1991; Merkle et al., 1996); 3) ion-exchange/adsorption (Taffarel and Rubio, 2009); 4) nanofiltration or reverse osmosis membrane filtration (Tobiason et al., 2016), and 5) microbial oxidation (Cerrato et al., 2010; Hoyland et al., 2014). Of these processes, adsorption and catalytic oxidation by using Mn oxide (MnOx)-coated media in the presence of free chlorine is often used because of its low cost, ease of operation, and stable removal efficiency (Singer and Reckhow, 2011). In this approach, Mn(II) is adsorbed on the surface of the MnOx, where it is catalytically oxidized by the free chlorine to produce new MnOx for subsequent Mn(II) removal (Knocke et al., 1991; Merkle et al., 1997). In a conventional water purification system composed of coagulation, flocculation, sedimentation, and media filtration processes, the filter media can be coated with MnOx, which allows for simultaneous removal of Mn(II) and suspended particles.

The use of microfiltration (MF) and ultrafiltration (UF) membrane filtration, which are solid–liquid separation processes for the removal of suspended matter from water, has increased in the past three decades, but these processes cannot remove Mn(II). To address this issue, a pre-ozonation process or a MnOx-coated media contactor with free chlorine can be added to the treatment process to oxidize and precipitate Mn(II). However, pre-ozonation has two problems: residual ozone may damage the membrane, and soluble hexavalent Mn, which cannot be removed by MF and UF, may be produced if ozone is added in excess. This means that in

practice a MnOx-coated media contactor is most often used because it uses the same chemical (chlorine) as used for disinfection, and, unlike ozone, chlorine does not produce soluble hexavalent Mn when added in excess.

However, setting up a contactor only for Mn(II) removal is not economical when the raw water contains Mn(II) at concentrations that do not have negative effects on health; that is, concentrations that are lower than the health-based maximum value (0.4 mg/L) presented by the World Health Organization (2017) but higher than the acceptable levels set for treated water (0.02 mg/L [Health Canada, 2019] and 0.05 mg/L [MHLWJ, 2002; USEPA, 2004]). It has also been reported that the accumulation of MnOx in distribution pipes and its release can result in stains forming on objects that the water comes into contact with and that these issues can occur at Mn(II) concentrations as low as 0.02 mg/L (Sly et al., 1990) and 0.01 mg/L (Li et al., 2019b). Therefore, water supply utilities usually set their own treatment targets for Mn(II) concentration. In Japan, many regional water supply utilities use a treatment target of ≤0.001 mg/L (for example, Kushiro City Water Supply and Sewerage Department, 2014; Moriwaki and Sakurai, 2012; Noboribetsu City Urban Development Department, 2019), which is much lower than the national limit of 0.05 mg/L, to prevent staining problems. Under these circumstances, a low-cost method for the removal of Mn(II) is desired.

Recently, Li et al. (2019a) reported that a commercially available powdered activated carbon (PAC) catalyzed Mn(II) oxidation in the presence of free chlorine and increased the oxidation rate by two orders of magnitude at a PAC dose as low as 5 mg/L compared with oxidation by free chlorine alone. Previous studies had reported the adsorption of Mn(II) on activated carbon, but the reported adsorption capacities were insufficient for practical application (Mohan and Chander, 2001; Savova et al., 2003). Indeed, Li et al. (2019a) were able to obtain only 95 % removal of Mn(II) in tens of minutes with a carbon dosage of 5 mg/L, which is attractive but must be improved before a truly economical water treatment process can

be realized. Independent of the work of Li et al. (2019a), we discovered recently in a membrane filtration pilot plant experiment that Mn(II) was removed by superfine powdered activated carbon (SPAC) in the presence of free chlorine, and that the Mn(II) removal rate was high enough for practical application of this approach as a water treatment process. This is an interesting discovery, not only scientifically but also practically, as traditional approaches to drinking water treatment have avoided the simultaneous use of activated carbon and chlorine due to chlorine consumption and carbon oxidation (Crittenden et al., 2012; Gillogly et al., 1998; Ohno et al., 2008; Snoeyink and Suidan, 1975; Summers et al., 2011). It might be easy to imagine that the large specific surface area of SPAC, which is produced by micro-milling of conventionally sized PAC [a median diameter (D50): tens of micrometers] and composed of particles with D50 of no larger than a few micrometers (Ando et al., 2010; He et al., 2020; Matsui et al., 2011; Pan et al., 2016), contributes to the high removability of manganese. In order to clarify this phenomenon as a science-based technology, however, an in-depth analysis of the high removability needs to be conducted.

SPAC is already being used as a novel adsorbent in five water treatment plants in Japan because of its high adsorption capacity and faster adsorption kinetics compared with PAC, but here we discuss the discovery of a new utilization of SPAC in water treatment processes. We first describe the Mn(II) removal by SPAC in the presence of free chlorine that we observed in our membrane filtration pilot plant experiment. We discuss the removal kinetics based on experimental data obtained from batch experiments.

2. Materials and Methods

2.1. *Activated carbons*

Two commercially available wood-based PACs were obtained and designated PAC-P (PL-WPS; Dainen Co., Ltd., Hyogo, Japan) and PAC-T (Taiko W; Futamura Chemical Co., Ltd., Nagoya, Japan). SPAC and submicron SPAC (SSPAC) were produced by milling each PAC in wet-mill systems. PAC-P was milled to SPAC-P by using a one-pass beads mill (NVM-1.5; Aimex Co., Ltd., Tokyo, Japan), and then stored as a slurry at the site of the membrane filtration pilot plant experiments. PAC-T was milled to SPACs and SSPACs of different particle sizes (SPAC-$T_{1–5}$ and SSPAC-$T_{1–3}$) by using a closed chamber ball mill followed by a recirculating beads mill (LMZ015; Ashizawa Finetech Ltd., Chiba, Japan). The SPACs and SSPACs produced from the PAC-T were stored as a slurry made with pure water (1–2 % w/v) at 4 °C after vacuum conditioning to remove air from the pores of the activated carbons.

The true particle size distributions of the activated carbons were determined by means of a laser-light diffraction and scattering method (Microtrac MT3300EXII; MicrotracBEL Corp., Osaka, Japan) after the addition of a dispersant (Triton X-100; Kanto Chemical Co., Tokyo, Japan; final concentration, 0.08 % w/v) followed by ultrasonic dispersion. The as-is particle size distributions of the activated carbons were determined by the same method but without the dispersant and ultrasonic dispersion. The carbon particle concentrations at the time of measurement in the Microtrac were from 5–50 mg/L. Table 1 shows the D50 values of the true particle size distributions of the activated carbons.

2.2. *Membrane filtration pilot plant experiment*

2.2.1. Membrane filtration pilot plant system

The experiments were conducted at the membrane filtration pilot plant located at the Shiraikawa Water Purification Plant of the Sapporo Waterworks Bureau, Japan (Fig. 1). The pilot plant had two lines. Line A consisted of in-line coagulation and membrane filtration.

Coagulation was performed for a hydraulic retention time of 5 s in the pipe mixing. Line B consisted of SPAC dosing, pre-chlorination, coagulation, and membrane filtration. SPAC and chlorine were dosed to the raw water at almost the same point along the line, which was at a hydraulic retention time of approximately 1 min prior to the point of coagulant dosing. The hydraulic retention time for the coagulation in the pipe mixing of Line B was 3 min. Poly-aluminum chloride (basicity 50 %; Hokkaido Soda Co. Ltd, Tomakomai, Japan), SPAC-P, and NaOCl were used as the coagulant, SPAC, and chlorine, respectively.

The membrane module of Line A housed a ceramic monolith membrane element with full-scale plant specifications (nominal pore size, 0.1 μm; filtration area, 24 m^2; membrane diameter, 180 mm; membrane length 1500 mm; Metawater Co., Ltd., Tokyo, Japan), whereas that of Line B housed a membrane element for small-scale experiments (nominal pore size, 0.1 μm; filtration area, 0.4 m^2; membrane diameter, 30 mm; membrane length 1000 mm). Both membrane modules were operated in dead-end mode at a constant flow rate of 4.0 m/d (167 L/(m^2 h)) under positive pressure. Hydraulic backwash was conducted every 3.0 h at 500 kPa using filtrate water from the permeate side. Each backwash was followed by a 150-kPa air-blow from the feed-water side to remove the suspension inside the module.

Solution pH before filtration and residual free chlorine concentration in the filtrate were monitored and kept constant (pH 6.8 and 0.2 mg-Cl_2/L, respectively) by automated-dosing of H_2SO_4 and NaOCl with a feedback control system, and the data were stored continuously. During the experiments, samples of the raw water and Line A and B filtrates were periodically collected and analyzed for Mn(II) concentration.

2.2.2. Raw water quality

The pilot plant was used to treat the raw water used by the Shiraikawa Water Purification Plant, which is taken from the Toyohira River. The total organic carbon (TOC) concentration

in the raw water was determined by a combustion catalytic oxidation method (TOC-L CPH/CPN; Shimadzu Co., Kyoto, Japan). The concentrations of Mn(II) and aluminum were determined by inductively coupled plasma mass spectrometry (ICP-MS; HP-7800; Agilent Technologies, Inc., CA, USA). Ultraviolet absorbance at 260 nm (UV260) was determined by using an ultraviolet and visible spectrophotometer (U-1900; Hitachi High-Tech Science Corporation, Tokyo, Japan). Raw water samples were filtered through filter paper (No. 5C; Toyo Roshi Kaisha, Ltd., Tokyo, Japan) prior to ICP-MS analysis and through a cellulose acetate membrane filter with a nominal pore size of 0.45 μm (DISMIC 25CS045AN; Toyo Roshi Kaisha) prior to UV260 analysis. The characteristics of the raw water are listed in Table 2.

2.3. *Batch experiments*

A stock solution containing 200 mg/L of Mn(II) was prepared by dissolving $MnCl_2 \cdot 4H_2O$ (Guaranteed Reagent; FUJIFILM Wako Pure Chemical Corporation, Osaka, Japan) in 0.1 mol/L HCl solution prepared from pure water (Milli-Q Advantage A10; Merck KGaA, Darmstadt, Germany). The low acidity kept the Mn(II) in a soluble form. Prior to the Mn(II) removal experiments, a beaker (4-L capacity, made from transparent polyvinyl chloride) and a floating magnetic stirrer (Nalgene Suspended Magnetic Stir Bar; Thermo Fisher Scientific Inc., Massachusetts, USA) were soaked in a tank filled with 5 % v/v nitric acid to dissolve and remove any metal residual. The floating magnetic stirrer was used to prevent the activated carbon particles from rubbing the bottom of the beaker, which could reduce the particle size.

In the batch experiments, 2000 mL of pure water containing 0.4 mmol of carbonate buffer ($NaHCO_3$) was spiked with the Mn stock solution at 10, 50, or 500 μg/L with stirring at 400 rpm. After adjusting the pH to 7.0–7.1 by using HCl and NaOH solutions, one of the PACs, SPACs, or SSPACs was added to the beaker at 1.0 mg/L. Control experiments without activated

carbon or chlorine were also conducted. After mixing for 5 min, NaOCl solution was added at 0.2, 0.3, 1.0, or 2.0 mg-Cl_2/L, and the resulting suspension was mixed for a further 15 min. During mixing, the pH was monitored with a pH meter (HM-20P; DKK-TOA Corporation, Tokyo, Japan) and adjusted to 7.0–7.1 (unless otherwise noted) by the addition of HCl or NaOH solution as needed. Periodically, samples (40 mL) of the mixture were withdrawn, filtered through a hydrophilic polytetrafluoroethylene membrane filter with a nominal pore size of 0.2 μm (DISMIC 25HP020AN, Toyo Roshi Kaisha), and the concentrations of soluble manganese and free chlorine were measured by ICP-MS (HP-7700; Agilent Technologies) and the *N*,*N*-diethyl-*p*-phenylenediamine colorimetric method (DR 900; Hach Co., Colorado, USA), respectively. Residual chlorine concentration was determined to the value obtained by adding 0.01 mg/L to the measured value because the filtration decreased slightly the free chlorine concentration by 0.01 mg/L.

SPAC particles in the withdrawn water were collected on an aluminum oxide membrane filter with a pore size of 0.2 μm (Anopore; Cytiva, Massachusetts, USA), which had been coated with gold to a thickness of 100 nm. The particles on the filter were observed using a field-emission scanning electron microscope (acceleration voltage, 5 kV; magnification, 7500; signal, LEI; working distance, 8.0 mm; JSM-7400F, JEOL Ltd., Tokyo, Japan) and an energy-dispersive X-ray spectrometer (JED-2300 Analysis Station; JEOL).

3. Results and Discussion

3.1. *Manganese removal by SPAC and chlorine in pilot plant experiments*

First, we conducted experiments using a pilot plant that comprised two water treatment lines. Both lines included coagulant and membrane filtration, but Line B also included SPAC and chlorination processes, whereas Line A did not. The experiments were conducted twice

(Run 1, 1 mg/L; Run 2, 3 mg/L SPAC). During the runs, the two lines were operated simultaneously to treat the same raw water, and the concentration of manganese in the raw water and in the filtrates were determined periodically to evaluate removal performance (Fig. 2).

The manganese concentrations in the raw water and Line-A filtrate were comparable in both runs (15–30 μg/L), indicating that soluble manganese was not removed by coagulation and membrane filtration treatment alone. In contrast, the manganese concentration in the Line-B filtrate in both runs was much lower than that in the raw water and Line-A filtrate. The maximum manganese concentration in the Line-B filtrate across both runs was 4 μg/L (Run 1; SPAC dosage, 1 mg/L). In Run 1, the manganese removal rate remained within the range of 74–88 %, which was not very high, but those removal rates were attained with a SPAC and chlorine contact time of only 4 min. When the dosage of SPAC was increased to 3 mg/L (Run 2), removal rates >95 % were achieved, and manganese concentrations in the treated water were lower than the limit of detection (1 μg/L).

Although these findings showed that pretreatment with SPAC and chlorination resulted in a marked reduction in manganese concentration, it remained unclear whether this removal was the result of chlorine-mediated oxidation of Mn(II) to tetravalent Mn (Mn(IV)) (Civardi and Tompeck, 2015), adsorption of the Mn(II) on the surface of the SPAC (Akl et al., 2013; Jusoh et al., 2005), or a combination of the effects of both the SPAC and chlorine. Therefore, we next conducted a series of batch experiments to examine the removal mechanism and kinetics underlying the observed manganese removal.

3.2. *Oxidation of Mn(II) by SPAC and chlorine*

To determine whether the observed removal of Mn(II) was a result of the action of the chlorine alone, SPAC alone, or the combined action of both, we conducted a series of batch

255 experiments and examined the change of Mn(II) concentrations under three conditions: the
256 presence of SPAC alone (absence of chlorine), the presence of chlorine alone (absence of
257 SPAC), or the presence of both SPAC and chlorine. The initial Mn(II) concentration was 10
258 μg/L, and the dosages of SPAC and chlorine were 1.0 mg/L and 1.0 mg-Cl_2/L, respectively.
259 During the runs, the concentrations of Mn(II) and free chlorine in the filtrate were determined
260 periodically to evaluate removal performance (Fig. 3).

261 The use of either SPAC or chlorine alone resulted in almost no change in the Mn(II)
262 concentration (proportion of Mn(II) remaining at 15 min was >99 %). Thus, chlorine alone at
263 1.0 mg-Cl_2/L was not enough to oxidize the Mn(II), and even if the activated carbon had some
264 ability to adsorb Mn(II), that ability was insufficient to remove Mn(II) under these conditions.
265 In contrast, combination treatment with SPAC and chlorine resulted in a marked decrease in
266 the Mn(II) concentration. The 90 % removal rate that was achieved within 10 min indicated
267 that the removal of Mn(II) observed in the previous pilot plant experiment was due to a
268 synergistic effect between SPAC and chlorine. Mn removal rates were comparable in the pH
269 range from 6.8 to 7.8, including the pH under which the pilot plant experiments were conducted
270 (Fig. S1, SI).

271 Based on these findings, we hypothesized that Mn(II) was oxidized to Mn(IV) by chlorine
272 on the surface of SPAC (we later learned that Li et al. (2019a) had already reported this
273 phenomenon for PAC). To examine this hypothesis further, we further conducted the batch
274 experiments using combination pretreatment with SPAC and chlorine and collected samples of
275 the SPAC. Fig. 4 shows representative field-emission scanning electron microscope
276 photographs of the SPAC particles sampled during this experiment. When no Mn(II) or a low
277 initial Mn concentration (50 μg/L) was used, the appearance of the SPAC particles remained
278 unchanged (Fig. 4A and B). However, when a high initial Mn(II) concentration (500 μg/L) was
279 used, the SPAC particles were covered in protrusions (Fig. 4C).

To further examine the change in appearance of the sampled particles, we repeated the previous experiment but extended the Mn-chlorine-SPAC contact time to 120 min and used energy-dispersive X-ray spectroscopy mapping analysis to examine a representative particle sampled during the experiment (Fig. 5). Fig. 5A shows a field-emission scanning electron microscope image of the sampled particle. Higher elemental manganese signals were observed in the protrusions than in the body of the particle (Fig. 5B), whereas higher elemental carbon signals were observed in the body of the particle than in the protrusions (Fig. 5C). Elemental oxygen signals were also higher in the protrusions than in the particle body, but the difference between the signals was barely detectable. (Fig. 5D). Together, these observations indicated that Mn oxide had precipitated on the surface of the activated carbon. In addition, the protruding nature of the precipitate suggests that the Mn oxide induced further oxidation of the Mn(II) in an autocatalytic manner (Coffey et al., 1993; Nakanishi, 1967; Singer and Reckhow, 2011).

3.3. *Removal rate coefficient and its independence from Mn(II) and chlorine concentration*

We assumed that the removal of Mn by combination treatment with activated carbon and chlorine observed in the pilot plant and batch experiments followed the pseudo-first-order reaction kinetics of equation (1) because of the almost-perfect semi-logarithmic correlation between Mn(II) concentration and time (Fig. 3A). Thus,

$$r = -k\, C_{\mathrm{Mn(II)}} \qquad (1)$$

where r is the removal rate of Mn(II) [mmol/(L s)], k is the rate coefficient of the pseudo-first-order reaction (s^{-1}), and $C_{\mathrm{Mn(II)}}$ is the bulk-phase Mn(II) concentration (mmol/L).

Li et al. (2019a) have interpreted the pseudo-first-order reaction kinetics of Mn(II) removal from the perspective of chemical oxidation. However, we applied an external-film mass transfer model because this model has been widely used to describe Mn(II) removal by MnOx-coated filter media in the presence of chlorine in previous studies (Bierlein et al., 2015; Dashtban

Kenari et al., 2019; Merkle et al., 1997). These studies present the model equations in the form of removal kinetics using filter media, but the basic form of the reaction kinetics can be written as follows:

$$r = -k_{\mathrm{f}} \frac{A\, C_{\mathrm{S}}}{\rho} \left(C_{\mathrm{Mn(II)}} - C_{\mathrm{E,Mn(II)}} \right) \quad (2)$$

$$C_{\mathrm{E,Mn(II)}} = fun(q_{\mathrm{Mn(II)}}) \quad (3)$$

$$\frac{dq_{\mathrm{Mn(II)}}}{dt} = k_{\mathrm{f}} \left(C_{\mathrm{Mn(II)}} - C_{\mathrm{E,Mn(II)}} \right) - k_{\mathrm{Cl2}}\, q_{\mathrm{Mn(II)}} C_{\mathrm{Cl2}} \quad (4)$$

where k_{f} is the mass transfer coefficient (m/s), A is the specific external surface area of the catalytic oxidation media (m^2/m^3), C_{S} is the concentration of the catalytic oxidation media (g/m^3), ρ is the density of the catalytic oxidation media (g/m^3), $C_{\mathrm{E,Mn(II)}}$ is the Mn(II) concentration in equilibrium with adsorbed-phase Mn(II) (mmol/L), $q_{\mathrm{Mn(II)}}$ is the mass of adsorbed-phase Mn(II) per unit of media surface (mol/m^2), $C_{\mathrm{E,Mn(II)}} = fun(q_{\mathrm{Mn(II)}})$ is the equilibrium relationship between the bulk liquid-phase and adsorbed-phase Mn(II) concentrations, t is time (s), k_{Cl2} is the oxidation reaction rate coefficient [$m^3/(mol\ s)$], and C_{Cl2} is chlorine concentration (mol/m^3).

If a similar model of equations (2–4) is applicable to Mn(II) removal by activated carbon in the presence of chlorine, our observation of the semi-logarithmic correlation would suggest the following condition: $C_{\mathrm{Mn(II)}} \gg C_{\mathrm{E,Mn}}$. This condition holds when $C_{\mathrm{Mn(II)}}$ is small relative to C_{Cl2} because $q_{\mathrm{Mn(II)}}$ and $C_{\mathrm{E,Mn}}$ are kept small according to equation (4) and (3), respectively. If equation (1) holds under this condition:

$$r \cong -k_{\mathrm{f}} \frac{AC_{\mathrm{S}}}{\rho}\, C_{\mathrm{Mn(II)}} = -k_{\mathrm{C}}\, C_{\mathrm{S}} C_{\mathrm{Mn(II)}} = -k\, C_{\mathrm{Mn(II)}}$$

328 (5)

329 where k_C is the carbon-dosage-normalized rate coefficient of the pseudo-first-order reaction
330 [L/(mg s)]. Thus, according to equation (5), the rate coefficients k and k_C should be independent
331 of Mn(II) and chlorine concentrations.

332 To confirm this hypothesis, we experimentally investigated the effects of Mn(II) and
333 chlorine concentrations on the rate of Mn(II) removal. First, the effect of initial Mn(II)
334 concentration on Mn(II) removal was examined using three initial Mn(II) concentrations (10,
335 50, and 500 μg/L) and 6 different activated carbons (Fig. 6 and Fig. S2, SI). When low initial
336 Mn(II) concentrations were used (10 and 50 μg/L), the changes in the proportion of Mn(II)
337 remaining were comparable and were fitted with similar k_C values. However, when a high initial
338 Mn(II) concentration was used (500 μg/L), the change in the proportion of Mn(II) remaining
339 was slower than the changes at the low initial concentrations. These results indicate that the
340 condition discussed above was actually held at low initial Mn(II) concentration but not at high
341 Mn(II) concentration. At high Mn(II) concentrations $q_{\mathrm{Mn(II)}}$ becomes large, such that the
342 condition $\left(C_{\mathrm{Mn(II)}} \gg C_{\mathrm{E,Mn}}\right)$ does not hold, and the overall removal rate is lowered. In addition,
343 we hypothesize that at high Mn(II) concentrations, a large amount of Mn(II) is precipitated on
344 the surface of the activated carbon, entirely covering the surface in a short period of time and
345 resulting in the Mn(II) being removed by the precipitated Mn oxide rather than the activated
346 carbon. Indeed, field-emission scanning electron microscopy analysis revealed visible Mn(II)
347 precipitation when a high initial Mn(II) concentration was used (Fig. 4C) but not when a low
348 initial Mn(II) concentration was used (Fig. 4B).

349 Next, we examined the effect of chlorine concentration on reaction rate by examining the
350 relationship between k_C and chlorine concentration (Fig. 7). k_C was used as an index of reaction
351 rate because of the semi-logarithmic correlation between Mn(II) concentration and time, as
352 described previously in Section 3.3. Because the residual free chlorine concentration gradually

353 decreased with time due to chlorine reductions in association with the SPAC present (Fig. 3B),
354 the residual free chlorine concentrations during the reaction were examined. When the initial
355 Mn(II) concentration was 10 μg/L, k_C did not change with chlorine concentration. In contrast,
356 when the initial Mn(II) concentration was 50 μg/L, k_C tended to decrease as the chlorine
357 concentration decreased; however, little change in the reduction of Mn(II) concentration was
358 observed (Fig S3, SI). Thus, we conclude that the dependence of k_C on chlorine concentration
359 was small, confirming our prediction that k and k_C would be independent of chlorine
360 concentration when equation (5) was derived from equations (2) to (4). Bierlein et al. (2015)
361 and Knocke et al. (2010) have reported similar results for the effect of free chlorine
362 concentration on the removal of Mn(II) by MnOx. Li et al. (2019a) have also reported no change
363 in the Mn(II) removal rate at chlorine doses of 1 to 4 mg/L. However, it does not mean no
364 requirement of chlorine for the Mn(II) removal. Mn(II) was not removed without chlorine (Fig.
365 3A). Therefore, there may exist a minimal chlorine concentration for the removal. Further
366 examinations of the role played by free chlorine in the removal of Mn(II) by activated carbon
367 are needed. This may be elucidated more quantitatively by identifying the parameters of
368 Equations 2-4 and the reaction equations of chlorine and activated carbon and solving these
369 equations simultaneously.
370
371 3.4. *Effect of activated carbon particle size on the removal of Mn(II)*
372 As shown in Fig. 6, the Mn(II) removal rates of SPAC-T_4, SPAC-T_3, and PAC-T differed
373 greatly, suggesting that the particle size of the activated carbon had a marked effect on the
374 Mn(II) removal rate. The data also suggested that removal of Mn(II) at a level suitable for real
375 world use (e.g., >97 % removal within 10 min) could be achieved by using 1 mg/L of one of
376 the SPACs, but not by using the PAC because the removal rate was too slow. To further examine
377 the effect of activated carbon particle size on the reaction rate, we conducted batch experiments

using nine activated carbons with different particle sizes (Table 1) and two initial concentrations of Mn(II) (10 or 50 μg/L). Plots of reaction rate parameters versus activated carbon particle size are shown in Fig. 8. The changes of Mn(II) concentration over time in each experiment are shown in Fig. S4 (SI).

First, when k_C was plotted against the median diameter of the true particle size distribution (true D50), k_C was found to increase with decreasing activated carbon particle size (Fig. 8A, circles and triangles). Decreasing the true D50 from 30 to 1.0 μm resulted in an increase of k_C by approximately 20 times. The k_C value of 1.0-μm SPAC was larger than the k_C value of 30-μm PAC (0.006 L/(mg s) vs. 0.0003 L/(mg s)).

Next, the data from the pilot experiment (see Section 3.1) and Li et al. (2019a) were fitted to equation (5), and the obtained k_C values were added to Fig. 8A. The k_C values of the pilot experiment were higher than those of the batch experiments, and the k_C values reported by Li et al. (2019a) were lower than those of the batch experiment. We had expected the k_C values obtained from equation (5), which assumes that external-film mass transfer is the rate-determining step, to be different between experiments because of differences in the stirring and mixing conditions used, but we were surprised to find that the values were somewhat comparable, indicating that the turbulence intensities in our batch experiment, our pilot plant experiment, and the batch experiment of Li et al. (2019a) were coincidentally similar. Most importantly though, the data clearly showed that micro-milling improved the Mn(II) removal efficiency of activated carbon.

When the true D50 was decreased from 30 to 1 μm, the rate of increase of k_C was reduced, and the k_C values remained at a constant value when the true D50 was less than 1 μm. Bonvin et al. (2016) and Pan et al. (2016) have reported that carbon particles in suspension can exist as aggregates rather than as discrete particles. We therefore hypothesized that the SPACs used in the Mn(II) removal experiments were aggregated and examined this hypothesis by measuring

403 as-is particle sizes, which were determined without any pretreatment, and comparing them with
404 the true particle sizes (Fig S5, SI). The true and as-is D50 values were comparable for the four
405 largest activated carbons, but not for the remaining smaller activated carbons, for which the as-
406 is D50 was much larger than the true D50, indicating marked aggregation. That is, the as-is D50
407 did not change even though the true D50 was decreased to the submicron range by the micro-
408 milling.

409 Then, we plotted k_C versus as-is D50 (Fig. 8B) and found a fairly strong linear relationship
410 (R^2 = 0.93), suggesting that particle aggregation was the primary reason why k_C remained
411 unchanged when plotted against the true D50 of the activated carbon in the submicron range.
412 This is reasonable because the external-film mass transfer model behind the pseudo-first-order
413 reaction kinetics (see Section 3.3) implicitly assumes that the rate-determining step of the
414 overall Mn(II) removal kinetics is mass transfer from the bulk liquid to the external surface of
415 the activated carbon particles. If the external-film mass transfer is the rate-determining step, the
416 overall reaction rate coefficient should vary with the as-is particle size, or more precisely with
417 the external surface area. In contrast, if the rate-determining step is the chemical oxidation
418 reaction on the activated carbon surface, the overall reaction rate coefficient should vary with
419 the true particle size rather than with the as-is particle size. The higher correlation of the overall
420 reaction rate coefficient with as-is D50 (Fig. 8B) compared with true D50 (Fig. 8A) strongly
421 suggests that the external-film mass transfer, not the chemical oxidation reaction, is the rate-
422 determining step.

423 Finally, we calculated the specific apparent external surface area of the activated carbon
424 particles using the as-is particle size distribution and then calculated the values of the mass
425 transfer coefficient (k_f) according to equation (5). Similar to what was found for k_C, k_f was found
426 to change with increasing as-is D50 (Fig. S6, SI). Many correlation equations that include the
427 relationship between k_f values and particle sizes have been proposed for mass transfer to

particles in agitated water, among which Armenante and Kirwan (1989) proposed the following correlation equation for microparticles:

$$\mathrm{Sh} \equiv \frac{k_\mathrm{f} d}{D_\mathrm{W}} = 2 + 0.52 \left(\frac{d^{4/3} \epsilon^{1/3}}{\sigma} \right)^{0.52} \left(\frac{\sigma}{D_\mathrm{W}} \right)^{1/3} \quad (6)$$

where Sh is the Sherwood number (dimensionless), d is the diameter of the microparticles (m), D_W is the diffusion coefficient in water (m^2/s), ε is the power input per mass of water (m^2/s^3), and σ is the kinematic viscosity (m^2/s). This equation tells us that the value of Sh minus 2 varies in proportion to the 0.69th power of the particle size.

Fig. 8C shows a plot of Sh minus 2 versus as-is D50 for our data. To determine the Sh value, the diffusion coefficient of hydrated Mn(II) ions in water was obtained from the works of Buffle et al. (2007) and Patil et al. (1991, 1982), and the density of activated carbon was obtained from the work of Pan et al. (2016). A fairly good positive correlation with a slope of 0.83 was observed, which is larger than the predicted slope of 0.69. Our data were obtained for less-spherical particles with a wider particle size distribution (Fig. S7, SI) than those used to derive equation (6); therefore, we consider the fit to be good for a dimensionless number correlation of this kind. Overall, the general trend that for small particles (diameter < 100 μm), mass transfer coefficient increase with the decrease in particle size was held in our data (Fig. S6, SI) (Upadhyay et al., 1994). Thus, these findings further support that the external-film mass transfer is the rate-determining step.

When interpreting the above results from a practical standpoint, a particle size of approximately 1–2 μm seems the most appropriate for Mn(II) removal because particles below 1 μm are severely aggregated, reducing removal efficiency (Fig. 8 and Fig. S5, SI). A wet-milling process was used in this study, but it is known that aggregation occurs more severely in

dry-milling processes (Pan et al., 2016). Therefore, the optimal particle size can vary depending on the applied milling system and condition. Even if activated carbon particles are aggregated, they could potentially have much faster Mn(II) removal if adequate dispersal could be achieved. Therefore, studies on milling and dispersion of SPAC to examine the potential for drinking water treatment are needed.

4. Conclusions

(1) Soluble Mn(II) was removed by SPAC in the presence of chlorine at feasible rates for practical application. In a pilot-scale membrane filtration experiment, within 4 min of contact with 3-mg/L SPAC, over 95 % of Mn(II) was removed, and a Mn(II) concentration less than the limit of detection (1 μg/L) was attained. Activated carbon was found to have a similar capability as Mn oxide for oxidative removal of Mn(II).

(2) The Mn(II) removal kinetics were well described by the pseudo-first-order reaction model by using the external-film mass transfer model. The carbon-dosage-normalized pseudo-first-order reaction rate coefficient value was independent of Mn(II) concentration, except at high Mn(II) concentrations, and was also independent of chlorine concentration.

(3) The carbon-dosage-normalized pseudo-first-order reaction coefficient increased in inverse proportion to the as-is particle size of activated carbon and in proportion to the specific apparent external surface area because the overall rate-determining step of Mn(II) removal was the external-film mass-transfer step. Practical removal of Mn(II) was found to be achievable with SPAC but not with PAC.

(4) The as-is size of the particles with a true size of less than 1–2 μm were almost constant because of particle aggregation. The carbon-dosage-normalized pseudo-first-order reaction coefficients were unchanged with true particle size for such particles. SPAC with a particle size

of around 1–2 μm was the most appropriate for Mn(II) removal. On the other hand, if effective dispersion processing of the aggregated particles is carried out in practice, a further increase in removal efficiency can be expected.

Acknowledgments

The authors gratefully acknowledge Futamura Chemical for providing the PAC samples (Nagoya, Japan). This work was supported by the Japan Society for the Promotion of Science [grant number JP16H06362]. The membrane filtration pilot experiment was part of the result of a joint research project of Sapporo Waterworks Bureau (Sapporo, Japan) and Metawater Co., Ltd. (Tokyo, Japan). However, the present work has not been evaluated by those entities and does not necessarily reflect their opinion; therefore, no official endorsement should be inferred.

References

Akl, M.A., Yousef, A.M., AbdElnasser, S., 2013. Removal of Iron and Manganese in Water Samples Using Activated Carbon Derived from Local Agro-Residues. J. Chem. Eng. Process Technol. 04. https://doi.org/10.4172/2157-7048.1000154

Ando, N., Matsui, Y., Kurotobi, R., Nakano, Y., Matsushita, T., Ohno, K., 2010. Comparison of natural organic matter adsorption capacities of super-powdered activated carbon and powdered activated Carbon. Water Res. 44, 4127–4136. https://doi.org/10.1016/j.watres.2010.05.029

Armenante, P.M., Kirwan, D.J., 1989. Mass transfer to microparticles in agitated systems. Chem. Eng. Sci. 44, 2781–2796. https://doi.org/10.1016/0009-2509(89)85088-2

Bierlein, K.A., Knocke, W.R., Tobiason, J.E., Subramaniam, A., Pham, M., Little, J.C., 2015. Modeling manganese removal in a pilot-scale postfiltration contactor. J. Am. Water Works Assoc. 107, E109–E119. https://doi.org/10.5942/jawwa.2015.107.0023

Bonvin, F., Jost, L., Randin, L., Bonvin, E., Kohn, T., 2016. Super-fine powdered activated carbon (SPAC) for efficient removal of micropollutants from wastewater treatment plant effluent. Water Res. 90, 90–99. https://doi.org/10.1016/j.watres.2015.12.001

Buffle, J., Zhang, Z., Startchev, K., 2007. Metal flux and dynamic speciation at (Bio)interfaces. Part I: Critical evaluation and compilation of physicochemical parameters for complexes with simple ligands and fulvic/humic substances. Environ. Sci. Technol. 41, 7609–7620. https://doi.org/10.1021/es070702p

Carlson, K.H., Knocke, W.R., Gertig, K.R., 1997. Optimizing treatment through Fe and Mn fractionation. J. / Am. Water Work. Assoc. 89, 162–171. https://doi.org/10.1002/j.1551-8833.1997.tb08216.x

Cerrato, J.M., Falkinham, J.O., Dietrich, A.M., Knocke, W.R., McKinney, C.W., Pruden, A., 2010. Manganese-oxidizing and -reducing microorganisms isolated from biofilms in chlorinated drinking water systems. Water Res. 44, 3935–3945. https://doi.org/10.1016/j.watres.2010.04.037

Civardi, J., Tompeck, M., 2015. Iron and manganese removal handbook, American Water Works Association.

Coffey, B.M., Gallagher, D.L., Knocke, W.R., 1993. Modeling Soluble Manganese Removal by Oxide-Coated Filter Media. J. Environ. Eng. 119, 679–694. https://doi.org/10.1061/(ASCE)0733-9372(1993)119:4(679)

Crittenden, J.C., Trussell, R.R., Hand, D.W., Howe, K.J., Tchobanoglous, G., 2012. MWH's Water Treatment: Princples and Design, third. ed. John Wiley & Sons, Inc., Hoboken, NJ, USA. https://doi.org/10.1002/9781118131473

526 Dashtban Kenari, S.L., Shabanian, J., Barbeau, B., 2019. Dynamic modeling of manganese
527 removal in a pyrolusite fluidized bed contactor. Water Res. 154, 125–135.
528 https://doi.org/10.1016/j.watres.2019.01.046
529 Gillogly, T.E.T., Snoeyink, V.L., Holthouse, A., Wilson, C.M., Royal, E.P., 1998. Effect of
530 chlorine on PAC's ability to adsorb MIB. J. / Am. Water Work. Assoc. 90, 107–114.
531 https://doi.org/10.1002/j.1551-8833.1998.tb08382.x
532 Gregory, D., Carlson, K., 2003. Effect of soluble Mn concentration on oxidation kinetics. J. /
533 Am. Water Work. Assoc. 95, 98–108. https://doi.org/10.1002/j.1551-
534 8833.2003.tb10273.x
535 He, H., Di, G., Gao, X., Fei, X., 2020. Use mechanochemical activation to enhance interfacial
536 contaminant removal: A review of recent developments and mainstream techniques.
537 Chemosphere 243, 125339. https://doi.org/10.1016/j.chemosphere.2019.125339
538 Health Canada, 2019. Guidelines for Canadian Drinking Water Quality: Guideline Technical
539 Document – Manganese, The Federal-Provincial-Territorial Committee on Drinking
540 Water. Ottawa, ON, Canada.
541 Hoyland, V.W., Knocke, W.R., Falkinham, J.O., Pruden, A., Singh, G., 2014. Effect of
542 drinking water treatment process parameters on biological removal of manganese from
543 surface water. Water Res. 66, 31–39. https://doi.org/10.1016/j.watres.2014.08.006
544 Islam, A.A., Goodwill, J.E., Bouchard, R., Tobiason, J.E., Knocke, W.R., 2010.
545 Characterization of filter media MnOX(S) surfaces and Mnremoval capability. J. / Am.
546 Water Work. Assoc. 102, 71–83. https://doi.org/10.1002/j.1551-8833.2010.tb10188.x
547 Jusoh, A., Cheng, W.H., Low, W.M., Nora'aini, A., Megat Mohd Noor, M.J., 2005. Study on
548 the removal of iron and manganese in groundwater by granular activated carbon.
549 Desalination 182, 347–353. https://doi.org/10.1016/j.desal.2005.03.022

Knocke, W.R., Occiano, S.C., Hungate, R., 1991. Removal of soluble manganese by oxide-coated filter media. Sorption rate and removal mechanism issues. J. / Am. Water Work. Assoc. 83, 64–69. https://doi.org/10.1002/j.1551-8833.1991.tb07201.x

Knocke, W.R., Zuravnsky, L., Little, J.C., Tobiason, J.E., 2010. Adsorptive contactors for removal of soluble manganese during drinking water treatment. J. / Am. Water Work. Assoc. 102, 64–75. https://doi.org/10.1002/j.1551-8833.2010.tb10171.x

Kushiro City Water Supply and Sewerage Department, 2014. The business requirement level of Aikoku Water Purification Plant Renewal Project, Kushiro City, Hokkaido, Japan (in Japanese). https://www.city.kushiro.lg.jp/common/000066158.pdf

Li, G., Hao, H., Zhuang, Y., Wang, Z., Shi, B., 2019a. Powdered activated carbon enhanced Manganese(II) removal by chlorine oxidation. Water Res. 156, 287–296. https://doi.org/10.1016/j.watres.2019.03.027

Li, G., Ma, X., Chen, R., Yu, Y., Tao, H., Shi, B., 2019b. Field studies of manganese deposition and release in drinking water distribution systems: Insight into deposit control. Water Res. 163. https://doi.org/10.1016/j.watres.2019.114897

Matsui, Y., Ando, N., Yoshida, T., Kurotobi, R., Matsushita, T., Ohno, K., 2011. Modeling high adsorption capacity and kinetics of organic macromolecules on super-powdered activated carbon. Water Res. 45, 1720–1728. https://doi.org/10.1016/j.watres.2010.11.020

Matsushita, T., Matsui, Y., Ikekame, S., Sakuma, M., Shirasaki, N., 2017. Trichloramine Removal with Activated Carbon is Governed by Two Reductive Reactions: A Theoretical Approach with Diffusion-Reaction Models. Environ. Sci. Technol. 51. https://doi.org/10.1021/acs.est.6b05461

Merkle, P.B., Knocke, W., Gallagher, D., Junta-Rosso, J., Solberg, T., 1996. Characterizing filter media mineral coatings: Characterizing filter media mineral coatings using

analytical techniques from geological science helps unlock fundamental filtration phenomena. J. / Am. Water Work. Assoc. 88, 62–73. https://doi.org/10.1002/j.1551-8833.1996.tb06662.x

Merkle, P.B., Knocke, W.R., Gallagher, D., Little, J.C., 1997. Dynamic Model for Soluble Mn2+ Removal by Oxide-Coated Filter Media. J. Environ. Eng. 123, 650–658. https://doi.org/https://doi.org/10.1061/(ASCE)0733-9372(1997)123:7(650)

MHLWJ, 2002. The water quality standards pursuant to the provision of Article 4 of the Waterworks Act, Ministry of Health, Labour and Welfare Government of Japan (MHLWJ) (in Japanese). https://www.mhlw.go.jp/shingi/2002/09/dl/s0904-4f2.pdf

Mohan, D., Chander, S., 2001. Single component and multi-component adsorption of metal ions by activated carbons. Colloids Surfaces A Physicochem. Eng. Asp. 177, 183–196. https://doi.org/10.1016/S0927-7757(00)00670-1

Moriwaki, K., Sakurai, K., 2012. Report on a Pilot Test of Water Purification Treatment at the Aikoku Water Purification Plant in Kushiro City, in: Proceedings of the 63rd National Symposium on Water Supply Research in Japan. pp. 242-245 (in Japanese).

Nakanishi, H., 1967. Kinetics of Continuous Removal of Manganese in a MnO2- Coated Sand Bed. Kogyo Kagaku Zasshi (Journal Chem. Soc. Japan) 70(4) (in Japanese).

Noboribetsu City Urban Development Department, 2019. The business requirement level of Noboribetsu Onsen Water Purification Plant Renewal Project, Noboribetsu City, Hokkaido, Japan (in japanese). https://www.city.noboribetsu.lg.jp/docs/2019040400020/file_contents/02.pdf

Ohno, K., Minami, T., Matsui, Y., Magara, Y., 2008. Effects of chlorine on organophosphorus pesticidesadsorbed on activated carbon: Desorptionand oxon formation. Water Res. 42, 1753–1759. https://doi.org/https://doi.org/10.1016/j.watres.2007.10.040

Pan, L., Matsui, Y., Matsushita, T., Shirasaki, N., 2016. Superiority of wet-milled over dry-milled superfine powdered activated carbon for adsorptive 2-methylisoborneol removal. Water Res. 102, 516–523. https://doi.org/10.1016/j.watres.2016.06.062

Patil, S.F., Adhyapak, N.G., Ujlambkar, S.K., 1982. Diffusion studies of manganese sulphate and manganese chloride in agar gel medium. Int. J. Appl. Radiat. Isot. 33, 1433–1437. https://doi.org/10.1016/0020-708X(82)90182-X

Patil, S.F., Rajurkar, N.S., Borhade, A. V., 1991. Self-diffusion of cobalt and manganese ions in aqueous electrolyte solutions. J. Chem. Soc. Faraday Trans. 87, 3405–3407. https://doi.org/10.1039/FT9918703405

Savova, D., Petrov, N., Yardim, M.., Ekinci, E., Budinova, T., Razvigorova, M., Minkova, V., 2003. The influence of the texture and surface properties of carbon adsorbents obtained from biomass products on the adsorption of manganese ions from aqueous solution. Carbon N. Y. 41, 1897–1903. https://doi.org/10.1016/S0008-6223(03)00179-9

Singer, P.C., Reckhow, D.A., 2011. Chapter 7 Chemical oxidation, in: Edzwald, J.., Association, A.W.W. (Eds.), Water Quality and Treatment: A Handbook on Drinking Water. McGraw-Hill.

Sly, L.I., Hodgkinson, M.C., Arunpairojana, V., 1990. Deposition of manganese in a drinking water distribution system. Appl. Environ. Microbiol. 56, 628–39. https://doi.org/10.2113/gsecongeo.26.8.799

Snoeyink, V.L., Suidan, M.T., 1975. Dechlorination by activated carbon and other reducing agents, in: Johnson, J.D. (Ed.), Disinfection: Water and Wastewater. Ann Arbor Science Publishers, pp. 339–358.

Summers, R.S., Knappe, D.R.U., Snoeyink, V.L., 2011. Chapter 14 Adsorption of organic compounds by activated carbon, in: Edzwald, J.K., Association, A.W.W. (Eds.), Water Quality and Treatment: A Handbook on Drinking Water. McGraw-Hill.

625 Taffarel, S.R., Rubio, J., 2009. On the removal of Mn2+ ions by adsorption onto natural and
626 activated Chilean zeolites. Miner. Eng. 22, 336–343.
627 https://doi.org/10.1016/j.mineng.2008.09.007
628 Tobiason, J.E., Bazilio, A., Goodwill, J., Mai, X., Nguyen, C., 2016. Manganese Removal
629 from Drinking Water Sources. Curr. Pollut. Reports 2, 168–177.
630 https://doi.org/10.1007/s40726-016-0036-2
631 Upadhyay, S.N., Rai, B.N., Kumar, V., Shah, Y.T., 1994. PARTICLE SUSPENSION AND
632 LIQUID-SOLID MASS TRANSFER IN MECHANICALLY AGITATED VESSEL.
633 Rev. Chem. Eng. 10, 1–130. https://doi.org/10.1515/REVCE.1994.10.1.1
634 USEPA, 2004. Drinking Water Health Advisory for Manganese, U.nited States
635 Environmental Protection Agency(USEPA), Office of Water, Washington DC, USA.
636 EPA-822-R-04-003.
637 WHO, 2017. Guidelines for drinking-water quality: fourth edition incorporating the first
638 addendum. World Health Organization, Geneva, Switzerland.

639

Table 1 True median diameters of the activated carbons after the addition of dispersant and ultrasonic dispersion pretreatment

Designation		True median diameter (μm)
Commercial PAC-P	PAC-P	15.4
	SPAC-P	1.24
Commercial PAC-T	PAC-T	29.3
	SPAC-T_1	10.1
	SPAC-T_2	4.85
	SPAC-T_3	2.68
	SPAC-T_4	1.51
	SPAC-T_5	0.79
	SSPAC-T_1	0.43
	SSPAC-T_2	0.17
	SSPAC-T_3	0.16

PAC: powdered activated carbon
SPAC: superfine powdered activated carbon
SSPAC: submicron superfine powdered activated carbon
PAC-P: PL-WPS (Dainen Co., Ltd., Hyogo, Japan)
PAC-T: Taiko W (Futamura Chemical Co., Ltd., Nagoya, Japan).

Table 2 Characteristics of the raw water used in the membrane filtration pilot plant experiments

	Temperature	Turbidity	UV260 *	TOC	pH	Mn *	Al *
	°C	NTU	abs/50 mm	mg/L		µg/L	mg/L
Run 1	7.1–11.6	5.1–9.9	0.11– 0.13	0.8–1.0	8.7–9.3	19–26	0.17–0.24
Run 2	14.1–20.1	1.5–1.9	0.11–0.14	0.9–0.9	7.3–8.3	16–27	0.09–0.09

*: analyzed after filtration

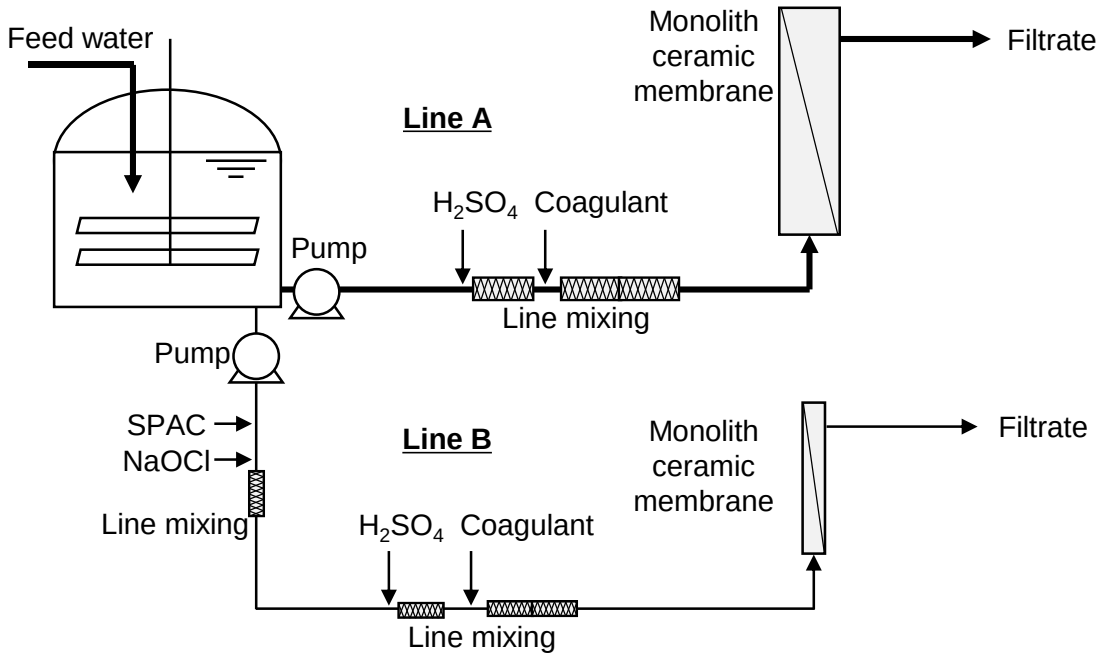

650

651 **Fig. 1.** Membrane filtration pilot plant system.

652

653

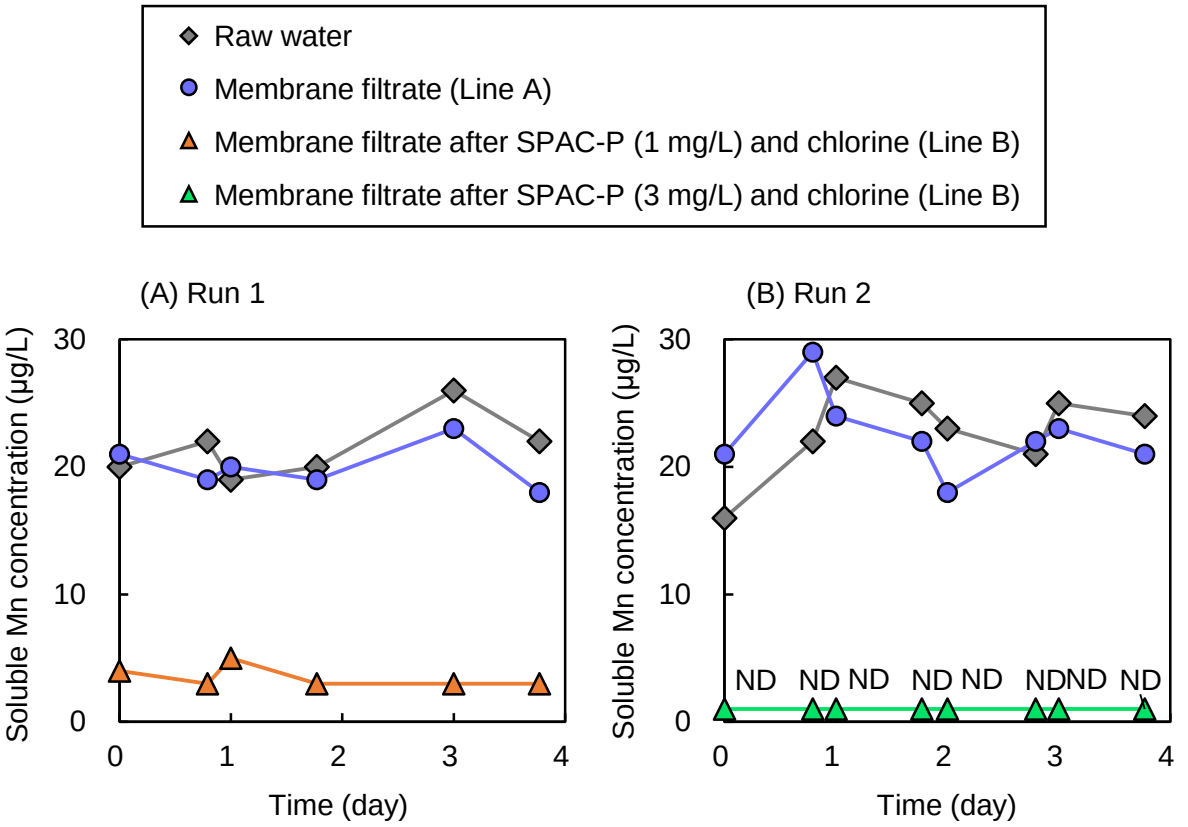

Fig. 2. Results of the pilot plant experiments examining the removal of soluble divalent Mn from raw water. The pilot plant comprised two treatment lines. Both lines included coagulant and membrane filtration, but Line B also included SPAC-P (D50 1.24 µm) and chlorination processes, whereas Line A did not. Two runs were conducted for each experiment with only the SPAC-P dosage differing between the runs. Chlorine dosage was controlled to maintain the residual free chlorine in membrane filtrate at 0.2 mg-Cl_2/L. ND, not detected (<1 µg/L).

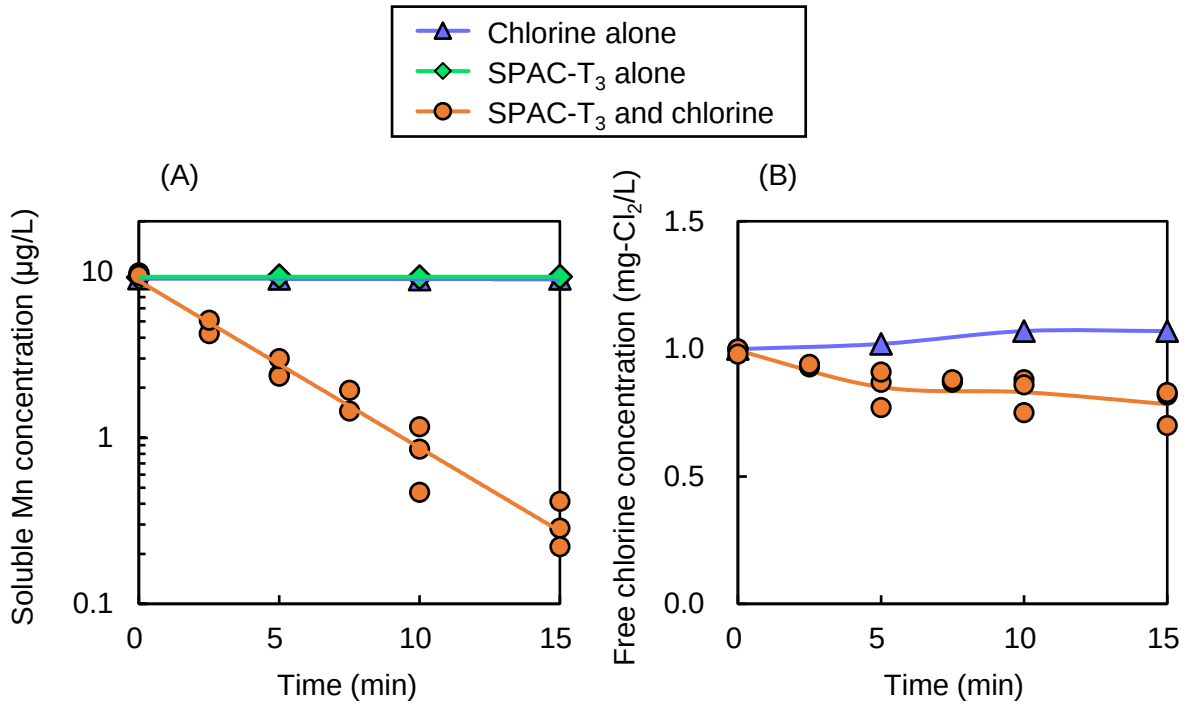

Fig. 3. Changes of soluble divalent Mn concentration (A) and free chlorine concentration (B) over time in the presence of chlorine alone, SPAC-T_3 (D50: 2.68 µm) alone, or both SPAC-T_3 and chlorine. Initial soluble divalent Mn concentration was 10 µg/L. Dosages of SPAC-T_3 and chlorine were 1.0 mg/L and 1.0 mg-Cl_2/L, respectively. Pure water containing carbonate buffer was used as the raw water.

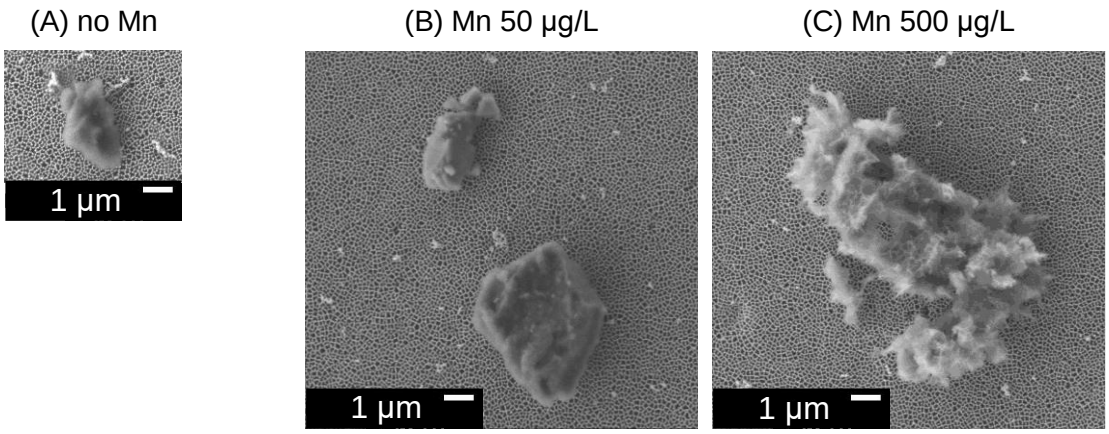

671

672 **Fig. 4.** Representative field-emission scanning electron microscopy images of SPAC-T_3 (D50:
673 2.68 µm) particles sampled during batch experiments using different initial
674 concentrations of soluble divalent Mn. Dosages of SPAC-T_3 and chlorine were 1.0
675 mg/L and 1.0 mg-Cl_2/L, respectively. Mn-chlorine-SPAC contact time was 60 min.
676 Pure water with carbonate buffer was used as the raw water. An alumina oxide
677 membrane filter with a 100-nm thick gold layer was used for particle collection.

678

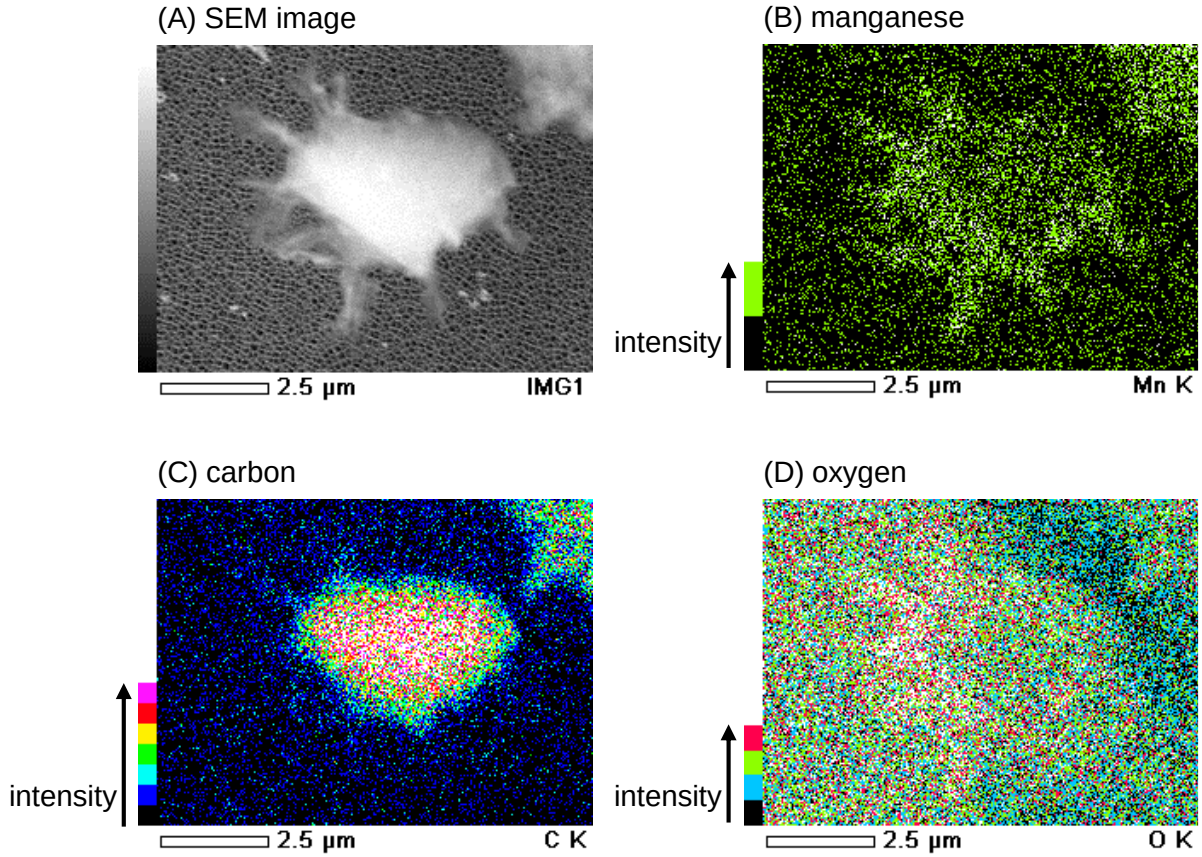

Fig. 5. Field-emission scanning electron microscopy (A) and energy-dispersive X-ray spectrometry mappings (B–D) of particles sampled from the batch experiment using combination pretreatment with SPAC-T_3 (D50: 2.68 µm) and chlorine and a high initial soluble divalent Mn concentration (500 µg/L). The dosages of SPAC-T_3 and chlorine were 1.0 mg/L and 1.0 mg-Cl_2/L, respectively. Mn-chlorine-SPAC contact time was 120 min. Pure water containing carbonate buffer was used as the raw water. An alumina oxide membrane filter with a 100-nm thick gold layer was used for particle collection.

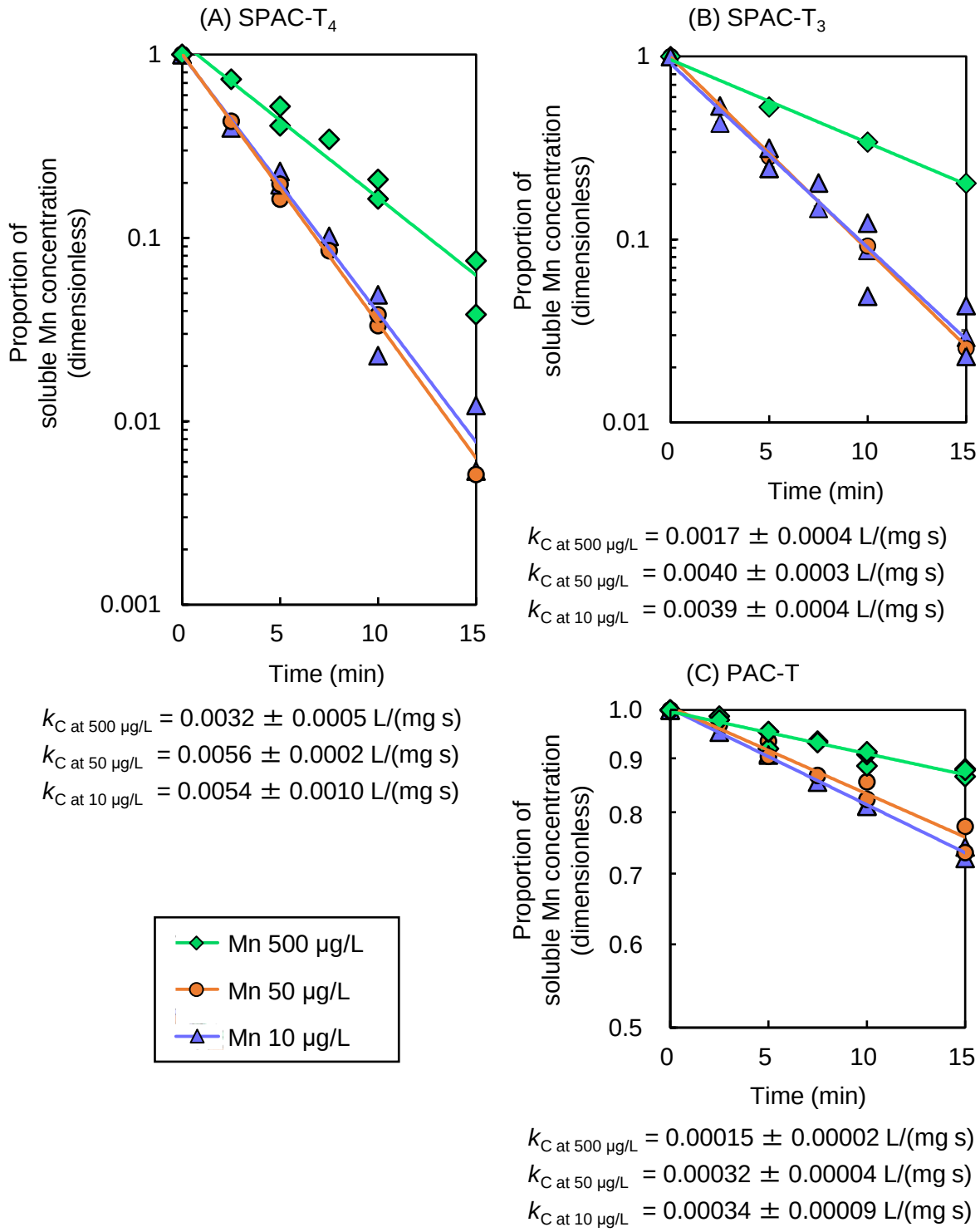

Fig. 6. Rate of soluble divalent Mn removal by SPAC-T_4 (D50: 1.51 µm) (A), SPAC-T_3 (2.68 µm) (B), and PAC-T (29.3 µm) (C) in the presence of chlorine at three initial Mn concentrations (10, 50, and 500 µg/L). The dosages of activated carbon and chlorine were 1.0 mg/L and 1.0 mg-Cl_2/L, respectively. Pure water containing carbonate buffer was used as the raw water. k_C is the carbon-dosage-normalized pseudo-first-order reaction rate coefficient obtained by semi-logarithmic correlation between Mn concentration and time, and the 95% confidence intervals of k_C are presented.

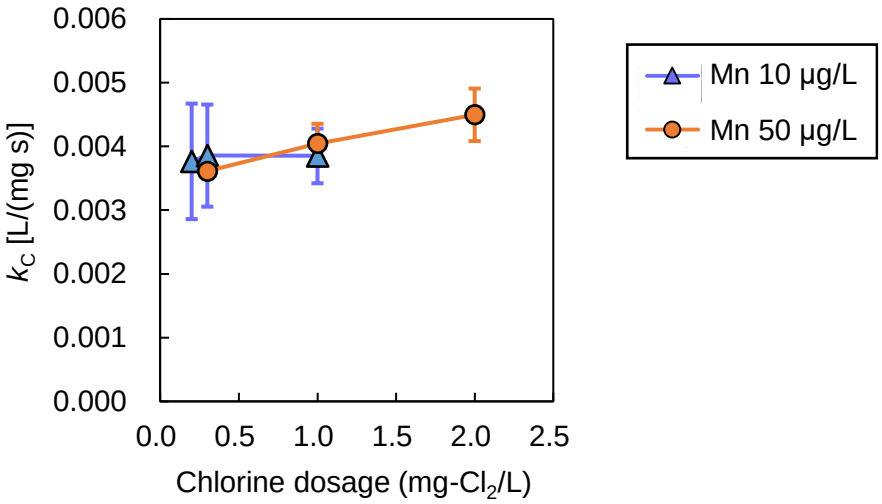

Fig. 7. Carbon-dosage-normalized pseudo-first-order reaction rate coefficient (k_C) versus chlorine dosage (A) and residual free chlorine concentration at 5 min (B). Experiments were conducted for two initial Mn concentrations (10 and 50 µg/L) and three chlorine dosages (data points moving left to right in both panels: 0.2, 0.3, and 1.0 mg-Cl_2/L with 10 µg-Mn/L; 0.3, 1.0, and 2.0 mg-Cl_2/L with 50 µg-Mn/L). SPAC-T_3 (D50: 2.68 µm) was applied at a dosage of 1.0 mg/L. Pure water containing carbonate buffer was used as the raw water. The changes of soluble divalent Mn concentration and free chlorine concentration with time are shown in Fig. 1S (SI). Error bars represent 95% confidence intervals.

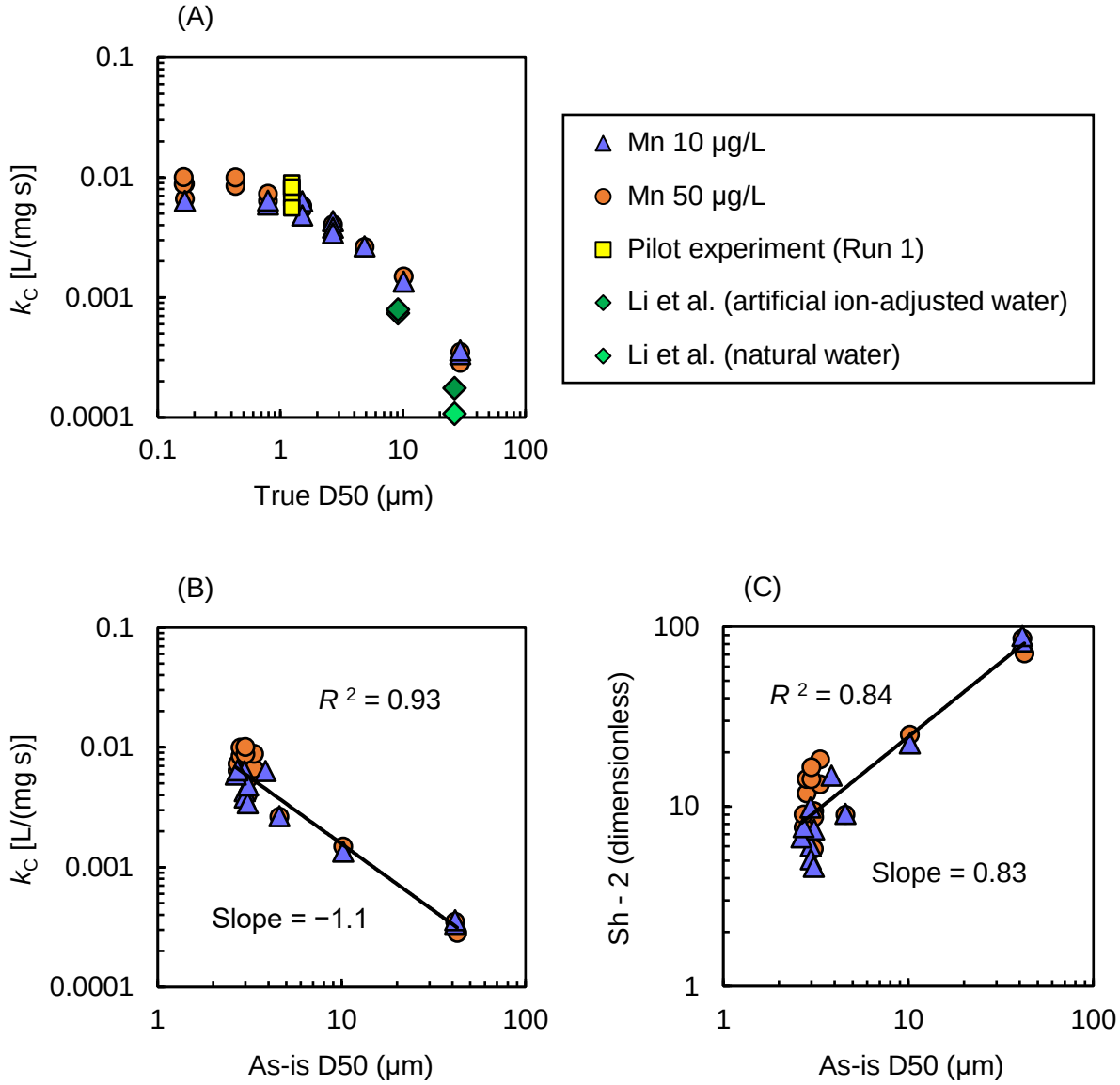

Fig. 8. Changes of reaction rate parameter values against activated carbon particle size. k_C is the carbon-dosage-normalized pseudo-first-order reaction rate coefficient. Sh is the Sherwood number. True D50 is the median diameter of particles in dispersed form. As-is D50 is the median diameter of particles in water without any dispersion treatment. Waters with two different initial Mn concentrations (10 and 50 μg/L) were used in the batch experiment. The dosages of activated carbon and chlorine were 1.0 mg/L and 1.0 mg-Cl_2/L, respectively. Pure water containing carbonate buffer was used as the raw water. The changes of soluble Mn concentrations over time in each batch are shown in Fig. 2S (SI). The data obtained in the pilot experiment discussed in Section 3.1 and those reported by Li et al. (2019a) are plotted in panel A.

Supplementary Materials

Oxidative removal of soluble divalent manganese ion by chlorine in the presence of superfine powdered activated carbon

Shun Saito [a, b], Yoshihiko Matsui [c*], Yasuhiko Yamamoto [b], Shuhei Matsushita [d], Satoru Mima [b], Nobutaka Shirasaki [c], and Taku Matsushita [c]

[a] Graduate School of Engineering, Hokkaido University, N13W8, Sapporo 060-8628, Japan

[b] METAWATER Co., Ltd., Kandasuda-cho 1-25, Chiyoda-ku, Tokyo 101-8554, Japan

[c] Faculty of Engineering, Hokkaido University, N13W8, Sapporo 060-8628, Japan

[d] School of Engineering, Hokkaido University, N13W8, Sapporo 060-8628, Japan

* Corresponding author. Tel./fax: +81-11-706-7280

E-mail address: matsui@eng.hokudai.ac.jp

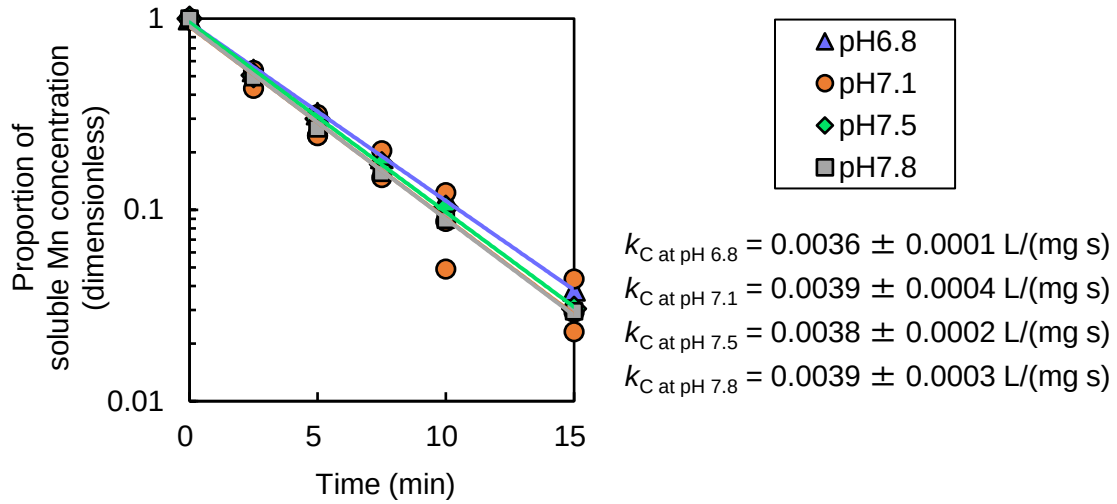

Fig. S1. Rate of soluble divalent Mn removal by SPAC-T_3 (D50 2.68 μm) in the presence of chlorine at four pH values (6.8, 7.1, 7.5, and 7.8). The dosages of SPAC-T_3 and chlorine were 1.0 mg/L and 1.0 mg-Cl_2/L, respectively. Pure water containing carbonate buffer was used as the raw water. k_C is the carbon-dosage-normalized pseudo-first-order reaction rate coefficient obtained by semi-logarithmic correlation between Mn concentration and time, and the 95% confidence intervals of k_C are presented.

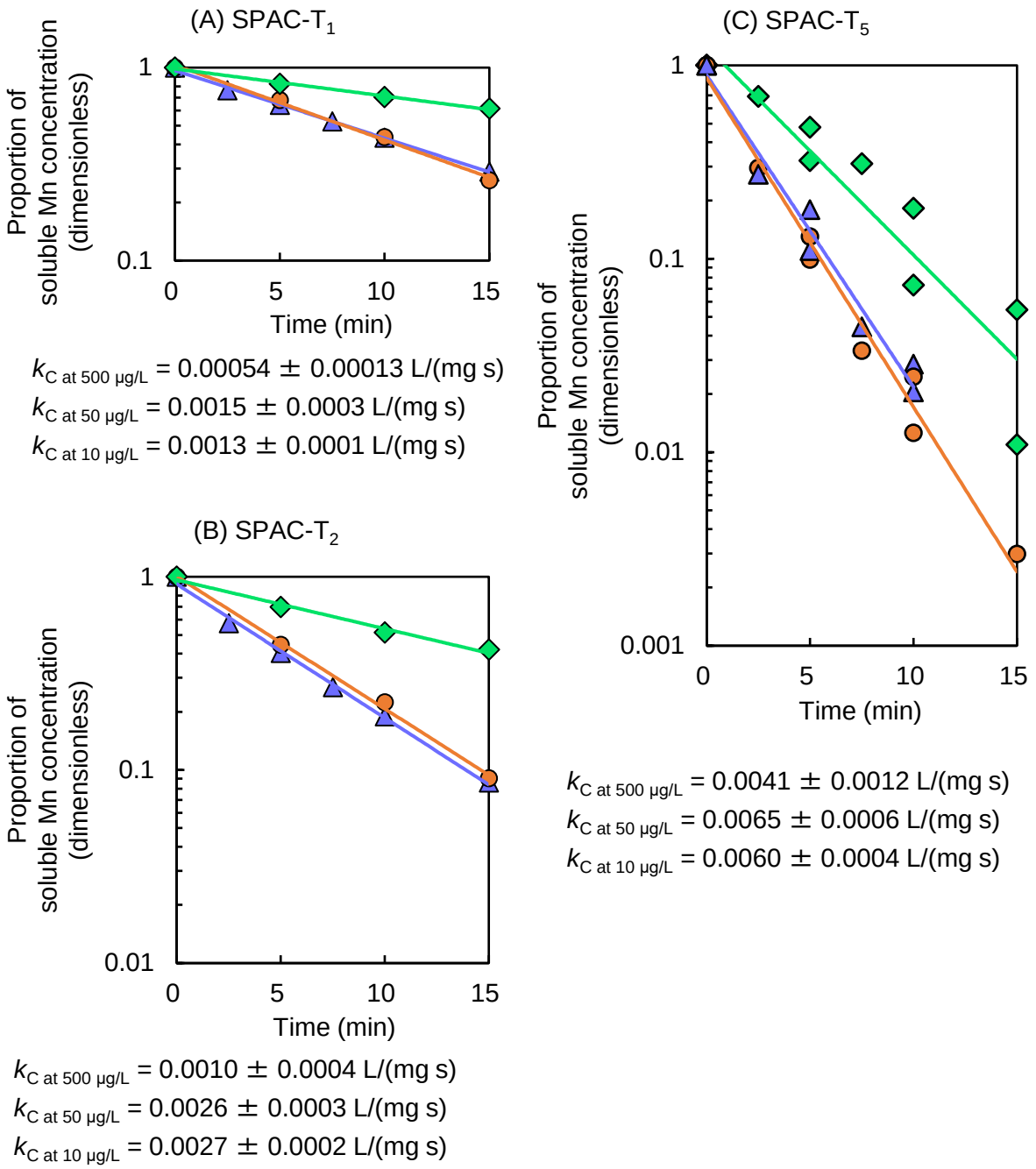

Fig. S2. Rate of soluble divalent Mn removal by SPAC-T_1 (D50 10.1 µm) (A), SPAC-T_2 (D50 4.85 µm) (B), and SPAC-T_5 (D50 0.79 µm) (C) in the presence of chlorine at three initial Mn concentrations (10, 50, and 500 µg/L). The dosages of activated carbon and chlorine were 1.0 mg/L and 1.0 mg-Cl_2/L, respectively. Pure water containing carbonate buffer was used as the raw water. k_C is the carbon-dosage-normalized pseudo-first-order reaction rate coefficient obtained by semi-logarithmic correlation between Mn concentration and time, and the 95% confidence intervals of k_C are presented.

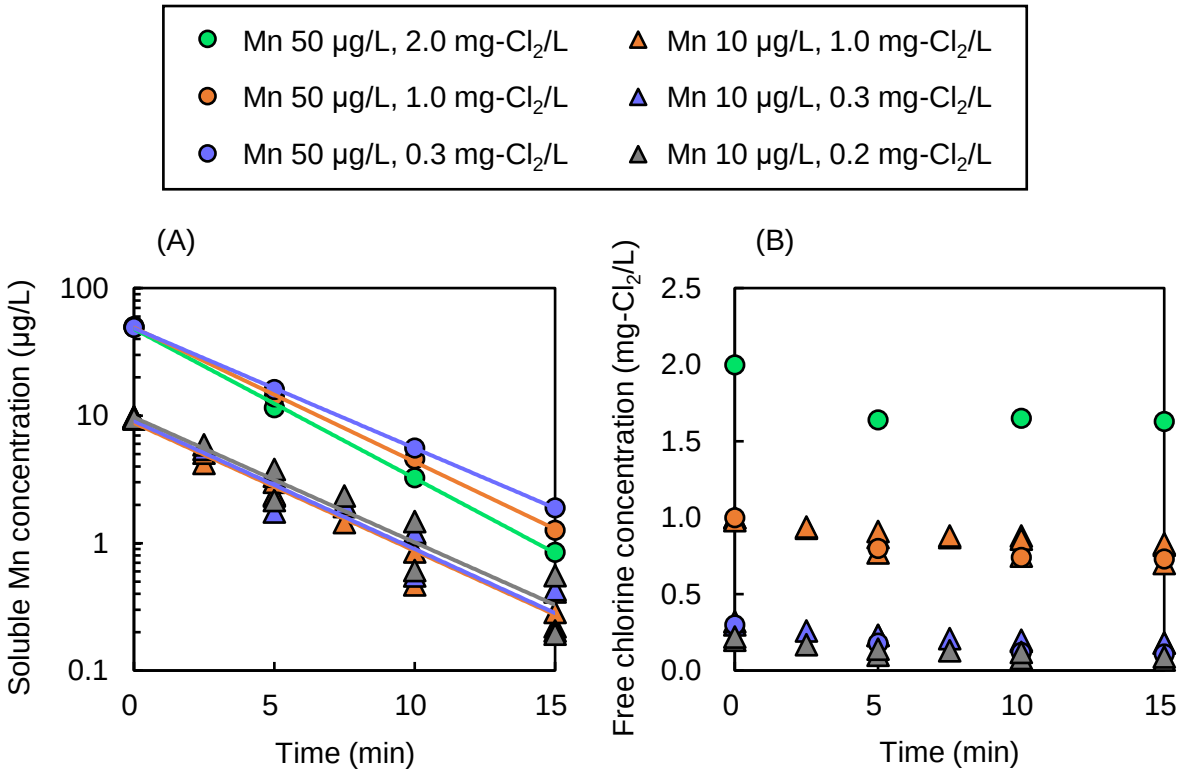

Fig. S3. Changes of soluble divalent Mn concentrations (A) and free chlorine concentrations (B) in batch experiments. Experiments were conducted for two initial Mn concentrations (10 and 50 µg/L) and three chlorine dosages. SPAC-T_3 (D50 2.68 µm)was used at a dosage of 1.0 mg/L. Pure water containing carbonate buffer was used as the raw water.

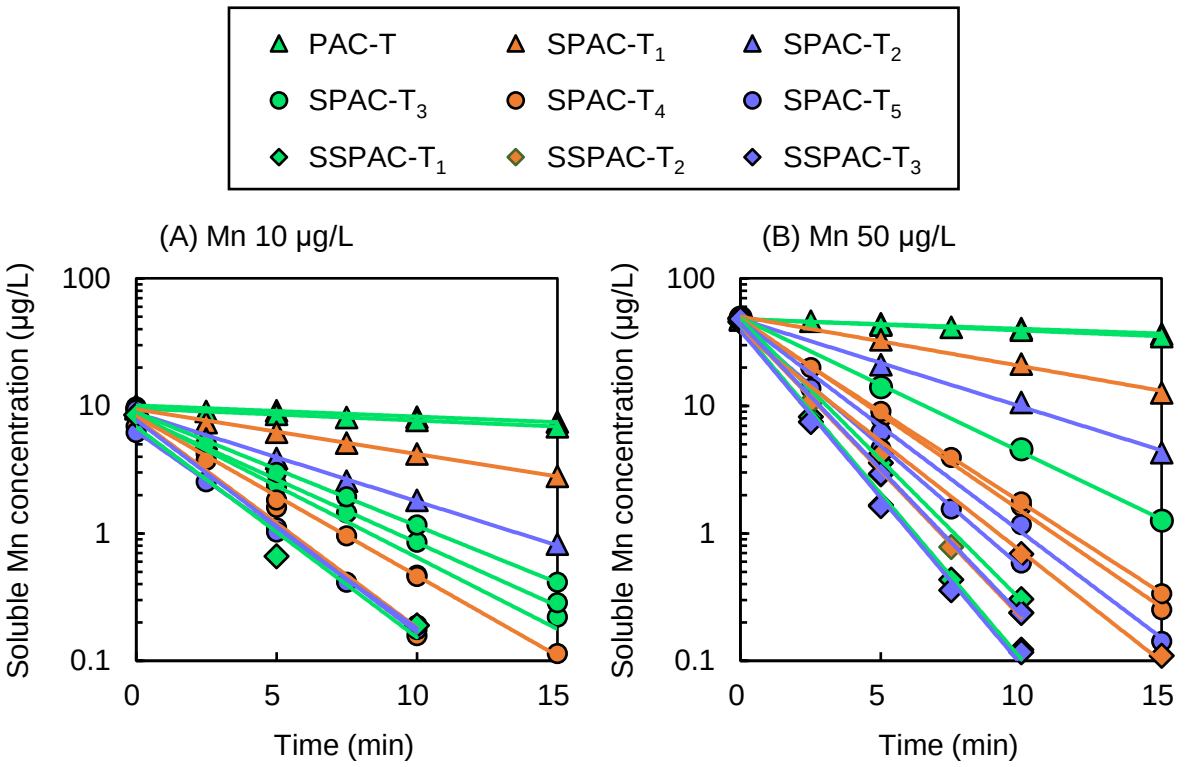

Fig. S4. Changes of soluble divalent Mn concentrations in batch experiments. Two initial Mn concentrations (10 and 50 μg/L) and nine activated carbons with different particle sizes were used. The dosages of activated carbon and chlorine were 1.0 mg/L and 1.0 mg-Cl_2/L, respectively. Pure water containing carbonate buffer was used as the raw water.

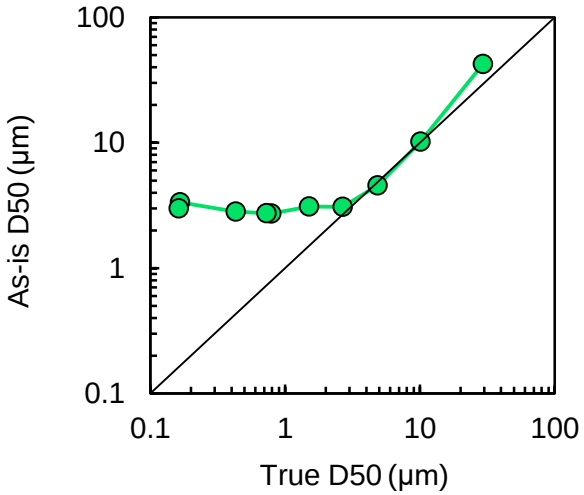

Fig. S5. Median diameters of the as-is particle size distributions (As-is D50) versus the true particle size distributions (True D50).

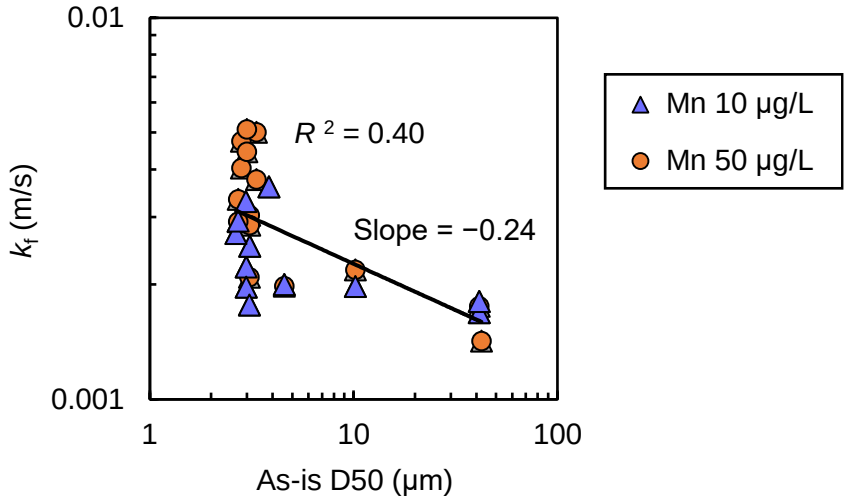

Fig. S6. Changes of mass transfer coefficient (k_f) against median diameters of the as-is particle size distributions (As-is D50). Waters with two different initial Mn concentrations (10 and 50 μg/L) were used in the batch experiment. The dosages of activated carbon and chlorine were 1.0 mg/L and 1.0 mg-Cl_2/L, respectively. Pure water containing carbonate buffer was used as the raw water. The changes of soluble Mn concentrations over time in each batch are shown in Fig. S4 (SI).

803
804

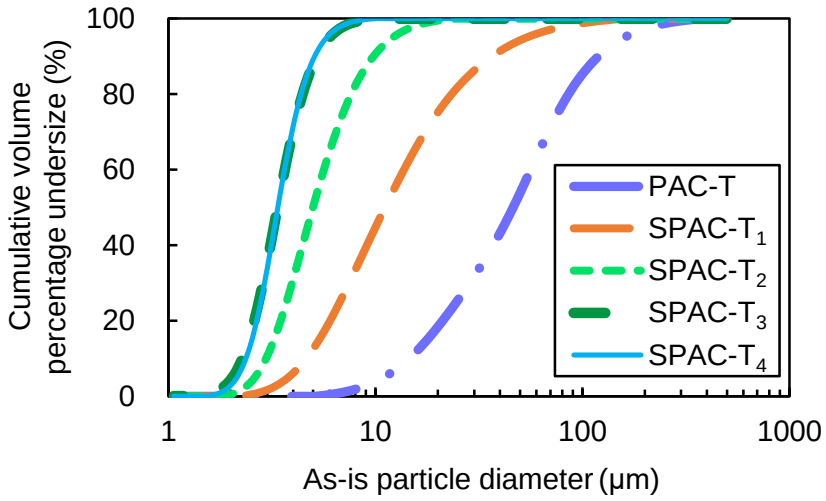

805

806 **Fig. S7.** As-is particle size distributions of selected activated carbons.